Dynamics of various Polymer/Graphene Interfacial Systems through Atomistic Molecular Dynamics Simulations

Anastassia Rissanou and Vagelis Harmandaris

Dynamics of various Polymer/Graphene Interfacial Systems through Atomistic Molecular Dynamics Simulations

Anastassia N. Rissanou[1,2*] and Vagelis Harmandaris[1,2,3*]

1. Department of Applied Mathematics, University of Crete, GR-71409, Heraklion, Crete, Greece.
2. Archimedes Center for Analysis, Modeling & Computation, University of Crete, P.O. Box 2208, GR-71003, Heraklion, Greece.
3. Institute of Applied and Computational Mathematics (IACM), Foundation for Research and Technology Hellas (FORTH), GR-71110 Heraklion, Crete, Greece.

Keywords: Molecular Dynamics simulations, polymer/graphene interactions, dynamical properties

Abstract

The current work refers to a simulation study on hybrid polymer/graphene interfacial systems. We explore the effect of graphene on the mobility of polymers, by studying three well known and widely used polymers, polyethylene (PE), polystyrene (PS) and poly(methyl-methacrylate) (PMMA). Qualitative and quantitative differences in the dynamic properties of the polymer chains in particular at the polymer/graphene interface are detected. Results concerning both the segmental and the terminal dynamics render PE much faster than the other two polymers, PS follows, while PMMA is the slowest one. Clear spatial dynamic heterogeneity has been observed for all model systems, with

* Author to whom correspondence should be addressed:
rissanou@tem.uoc.gr +30 2810393746 fax: +30 2810393701
vagelis@tem.uoc.gr +30 2810393735 fax: +30 2810393701

different dynamical behavior of the adsorbed polymer segments. The segmental relaxation time of polymer (τ_{seg}) as a function of the distance from graphene shows an abrupt decrease beyond the first adsorption layer for PE, as a result of its the well-ordered layered structure close to graphene, though a more gradual decay for PS and PMMA. The distribution of the relaxation times of adsorbed segments was also found to be broader than the bulk ones for all three polymer/graphene systems.

1 Introduction

The study of graphene based polymer nanocomposites is a very intense research area due to very broad possible applications of such systems.[1,2] Indeed, the properties of all polymer nanocomposites (PNC) can be tuned, by the proper selection of the solid phase, in order for the hybrid (composite) system to be used in various applications. This is of particular importance for graphene based PNC, because of the exceptional physical properties of graphene (e.g. electron transport capacity, electrical conductivity, high intrinsic tensile strength and stiffness, high thermal conductivity, etc.) which render this material as a promising candidate for the reinforcement of polymer nanocomposites.[1,2,3]

Considering all of the above, various experimental approaches have been used to study different aspects of polymer/graphene systems.[2,3,4,5,6,7,8,9,10,11] For example, the dispersion of graphene, graphene oxide or carbon nanotubes, into a polymer matrix has been shown to alter significantly the mechanical as well as rheological, electrical and barrier properties of pure polymers.[2,5] In this aspect the study of the polymer/graphene interface in the molecular level is *condicio sine qua non* in order to understand the behavior, and predict the properties, of the hybrid material. For experimental techniques the main difficulty lies in the detailed characterization of the polymer/graphene interface, which might be either too small to be resolved, or which is masked by the larger bulk region.[2,4]

Molecular simulation approaches can complement experiments by providing a detailed study of the polymer chains near the polymer/graphene interface. Atomistic molecular dynamics (MD) simulations are particularly important due to their capability of providing direct quantitative information about both structural and dynamical properties of the hybrid material. For this reason the last few years several simulation works concerning the properties of various polymer/graphene (or polymer/graphite) nanostructured systems were appeared in the literature.[12,13,14,15,16,17,18,19,20,21,22,23,24,25,26,27] The study of the dynamics of polymer chains close to graphene layers is of special importance, since friction at the interface determines the dynamical, the rheological as well as the mechanical properties of the hybrid system.

Molecular Dynamics (MD) and Monte Carlo (MC) simulations of polymer/graphite interfacial systems began to appear in the literature 2–3 decades ago.[12] Most of the early

work was concerned with very simple systems, such as alkane chains, or simple bead spring models.[12,13,28] Several simulation works of polymer/graphite systems in the past shown that segmental dynamics of the adsorbed molecules perpendicular to the surface is quantitatively and qualitatively different from that in the bulk and cannot be described by a constant diffusivity. It can, however, be accurately described using a macroscopic diffusion equation with a time-dependent diffusion coefficient, *D(t)*.[13]

All the above works show some similar characteristics concerning the behavior of the model polymer chains. However, the actual polymer/solid (graphene) interaction is expected to play a crucial role in the properties of the hybrid nanostructured material and in particular of the polymer chains at the interface. For example, it is now well recognized that the width of the polymer/solid interface depends on the actual polymer atom/solid atom pair interaction, the size of the polymer chains, as well as the actual property under study.[18,29,30,32] In addition recent simulations studies[31,32] examined large-scale equilibrium properties of the polymer/surface interface in melts, using coarse grained lattice and off-lattice models, where the typical lengths were exceeded the statistical segment length (i.e., Kuhn segment). Overall, despite the qualitative similarities on the properties of polymers at interfaces, a quantitative study of the structure and dynamics requires a detailed representation of the specific chemical interaction between the polymer and the surface.

With respect to the above discussion it is clear that comparative simulation works of different polymers can be a valuable tool in order to clarify (and quantify) the effect of the (graphene) solid phase on the properties of various (graphene) PNCs. This is exactly the scope of the present work: To provide a comparative, both qualitative and quantitative, study of the effect of the graphene layers on the dynamical properties of different polymeric systems. We choose three very common polymers, i.e. polyethylene (PE), polystyrene (PS) and polymethylmethacrylate (PMMA), which are used extensively in the application of graphene based polymer nanocomposites.[1,2] In the current work we focus on very shorter length scales of atomic level (i.e., very close to the surface).

This work is part of a more general hierarchical multi-scale simulation approach for the study of polymer/graphene (and more general polymer/solid) interfacial systems at multiple length and time scales. The structural and conformational characteristics of the

above model systems have been presented elsewhere.[18,19] Here we focus on the dynamical properties of the nanostructured model systems. In more detail, in the next Section we provide a short overview of the simulations and of the model systems. Results concerning both the segmental and the terminal (chain) dynamics of the polymer chains are presented in the third Section. Finally, our findings and conclusions are summarized in Section 4.

2 Systems and Simulation Method

In this work we present a detailed analysis of the dynamics of three different polymer/graphene systems, through atomistic Molecular Dynamics (MD) simulations. In more detail we study: a) PS/graphene, (b) PMMA/graphene and (c) PE/graphene interfacial systems, as well as the corresponding bulk polymer systems. For PS and PMMA polymer chains are *10*-mers, while PE chains consist of *22*-mers. Number of monomers was chosen in such a way that the backbone consists of almost the same number of CH_2, and/or CH, groups for all systems; i.e. PS and PMMA chains have 20 (CH_2 and CH) groups in the backbone, while PE has 22 CH_2 groups. This choice also leads to very similar mean sizes for the bulk polymer chains, as they are quantified by the average radius of gyration: $\langle R_g \rangle_{PS}=0.696nm$, $\langle R_g \rangle_{PMMA}=0.695nm$, $\langle R_g \rangle_{PE}=0.620nm$ for PS, PMMA and PE respectively. Error bars are about *5%* of the actual value. The reference bulk systems consist of *56 10*-mer chains for PS, *54 10*-mer chains for PMMA and *420 22*-mer chains for PE.

All simulations were carried out at constant temperature equal to $T=500K$ for PS and PMMA and T=450K for PE, using the stochastic velocity rescaling thermostat[33] and the GROMACS code.[34] We should state here that for PS and PMMA the actual temperature is almost equidistant from their glass transition temperatures (i.e. $T_g^{PS} \cong 360K$, and $T_g^{PMMA} \cong 380K$). But, this is not the case for PE, because the glass transition temperature of PE is much lower ($T_g^{PE} \cong 190K$) and an equidistant temperature from T_g^{PE} would lead to temperature values where PE is crystallized (i.e., $T\sim$ [*310-330*]K, while the melting point of PE is about *410K*). This aspect will be further discussed in the results section. For *NPT* simulations the pressure was kept constant at $P=1atm$, using a Berendsen barostat. An all atom representation model has been used, in which non-bonded interactions in PE are described by Lennard-Jones and Coulomb potentials. The

OPLS atomistic force field has been used for the description of the intermolecular and intramolecular interactions of PMMA[35] and PS.[36] For the interaction between polymer atoms and graphene layers the Lorentz-Berthelot rules have been used, i.e., arithmetic averages for the calculation of σ_{ij}: $\sigma_{ij} = (\sigma_{ii} + \sigma_{jj})/2$, while geometric averages for the calculation of ε_{ij}: $\varepsilon_{ij} = (\varepsilon_{ii}\varepsilon_{jj})^{0.5}$, where *i* and *j* are the types of polymer and graphene atoms respectively. Graphene has been represented as a set of LJ carbon atoms, centered at their crystallographic positions, whereas the parameters for the non-bonded interaction of the graphene carbons were taken from a potential used for graphite: $\varepsilon_{cc}/k_B=28K$ and $\sigma_{cc}=3.4\text{Å}$.[37] The lattice constant is that of graphite, equal to *2.462Å*. At this point, no interactions were assumed between graphene atoms, which remained fixed in space during the simulation. Note also that the analysis of test polymer/graphene runs, using a full (including intra-molecular terms) force field for graphene shown almost the same results for the structural and dynamical properties of the polymer matrix. However, the incorporation of a full intra-molecular force field for graphene layers is crucial if someone is particular interested in studying the effect of the polymer matrix on the properties of the graphene layers. This will be the subject of a following work.

Periodic boundary conditions have been used in all three directions, so that the polymer interacts with the graphene layer, which is placed at the bottom of the simulation box, on the *xy* plane, and its periodic image at the top of the simulation box simultaneously. This setup renders our systems polymer films confined between two graphene surfaces, i.e. assuming ideal dispersion of graphene sheets. This is certainly not the usual case for realistic nanocomposites[38], however we do not expect this assumption to introduce artifacts, since: (a) the width of the films is rather large and all the systems exhibit a clear bulk polymer region and, (b) we are particular interested in large (compared to chain size) graphene layers. Moreover, periodic boundary conditions ensure infinite graphene layers with no edges, which are eclectrically neutral. Atomistic MD simulations for all systems have been performed for times from *0.3* up to *0.5* μs. More details about the all-atom force field, as well as the MD simulations are given elsewhere.[18]

Setup details are depicted in Table 1, where *N* is the number of polymer chains in the simulation box and *d* is the film thickness. The film thickness is calculated from the

box length along the z-direction subtracting the thickness of the graphene layer, *0.34 nm* (i.e of the order of one van der Waals radius), which is placed at $z=0$. The number of the polymer chains in each system was chosen so that, in combination with the specific chain length, polymer films of almost equal thicknesses are formed. Concerning the bulk systems the *NPT* simulations predict an average density of $0.965 g/cm^3$ for the atactic PS, $1.054 g/cm^3$ for the atactic PMMA and $0.663 g/cm^3$ for the PE. These values are in very good agreement with experimental data as discussed before.[18,39,40]

3 Results and Discussion

The purpose of this study is to quantify the effect of the graphene surface on the chain dynamics for polymers with different molecular structure. This is essential if we consider that differences in the molecule/graphene interactions can lead to a much different dynamical behavior of the polymer chains, and consequently to different rheological as well as mechanical properties of the hybrid composite system. The molecular structure (i.e., polymer architecture), of the three polymers (PS, PMMA and PE) is shown in Figures 1a-c respectively.

The molecular density of the polymer chains at the polymer/graphene interface is of great importance for the properties of the hybrid system. Therefore, we have analyzed the density of the polymer chains, as a function of the distance from the graphene layer. In Figure 2 we present density profiles, based on the monomer center of mass, $\rho(z)$, for the three hybrid polymer/graphene systems studied here. First, the average density profiles show a high peak (maximum) in $\rho(z)$, around *0.4* nm from the graphene, for all polymer/graphene systems. This is not surprising if we consider that all polymers studied here are "physically" adsorbed on the graphene layers, i.e. the polymer/graphene interaction is primarily due to dispersion van der Waals force between polymer atoms and graphene carbons. Such a dense polymer layer close to a solid surface has been also observed in past simulations of polymer–solid interfaces with atomistic[12,13,21,24] as well as coarse-grained models.[28,41,42,43,44] However, there are slight quantitative differences among the three density profiles related to the value of the first peak of $\rho(z)$, which reveals the weakest attraction from the graphene layer on PE, while PMMA and PS feel a stronger attraction. On top of that, density profile of PE shows a characteristic oscillation

profile with two more substantially lower peaks. These peaks are related to the simpler molecular structure of PE (CH_2 groups along the backbone, with no side groups), compared to both PS and PMMA, that leads to chain conformations that form a well-ordered layered structure close to graphene.[18,19] Note that similar density oscillation profiles have been found from simulations of simple bead-spring models that also exhibit the same PE-like molecular structure.[28]

Second, density profiles are symmetrical with respect to the center of the film and attain their bulk density, almost in the middle of the polymer film as expected. The shape of the density profiles' curves reflects the specific setup of the simulated systems. Bulk density values show that PE has the smallest density; PS follows, while PMMA is the densest one. Overall, the slight differences in the density profiles further contribute, as it will be discussed below, to clear quantitative and qualitative differences in the dynamical properties of the different systems.

Furthermore, the strength of the overall interaction between the graphene layer and the polymer matrix can be quantified through the calculation of the "adsorption energy" for the three systems. This (potential) energy describes the average non-bonded dispersion (Lennard Jones) interaction between the surface and the amount of polymer which lies in a distance smaller than *1nm* (i.e. cutoff for LJ interactions) from graphene layer. For comparison reasons we present these values as energy per area and they are equal to: *-356.40±8.2 kJ/(mol nm$^{2)}$* for PE, *-434.48±16 kJ/(mol nm^2)* for PS and *-396.25±9.9 kJ/(mol nm^2)* for PMMA. In agreement with the picture of the density profiles, the smallest "adsorption energy" (in absolute value) is that of PE, the second one is that of PMMA while the largest is the one of PS.

The above findings concerning the density profiles predispose us for different diffusion processes among the three polymer/graphene systems. Therefore, below we examine in detail both the orientational and the translational dynamics of the polymer/graphene systems. A common way to describe the orientational mobility of polymer chains at various levels of analysis is through the use of time correlation functions of vectors, defined on a polymer chain. These vectors are usually defined either in the segmental (monomeric) level or in the polymer chain level (e.g. end-to-end vector).

In the current work both the first and the second-order bond order parameters (i.e. first, $P_1(t)$, and second, $P_2(t)$, Legendre polynomials) have been calculated through:

$$P_1(t) = \langle \cos\theta(t) \rangle, \qquad P_2(t) = \frac{3}{2}\langle \cos^2\theta(t) \rangle - \frac{1}{2}$$

In the above expressions $\theta(t)$ is the angle of the vector under consideration at time t relative to its position at $t=0$. Note that both $P_1(t)$ and $P_2(t)$ are quantities which can be directly related to experimental measurements. For example if a comparison of the atomistic simulations with dielectric spectroscopy is sought, $P_1(t)$ of the dipole moment vector should be calculated, whereas if someone is interested to compare MD data with ^{13}C and ^{2}H NMR relaxation measurements, $P_2(t)$ of the C-H bonds should be chosen.[46]

Concerning the translational dynamics of the polymer chains, a standard measure of their mobility is the mean square displacement of atoms (or of the center-of-mass) of the polymer chains, ΔR^2, calculated through:

$$\Delta R^2 \equiv \left\langle \left(R(t) - R(0) \right)^2 \right\rangle,$$

where $R(t)$ and $R(t)$ are the position of the atoms (or chain's center of mass) at time t and 0 respectively.

In the following we present results concerning the dynamics of polymer chains, using the above mentioned quantities, for both the segmental (i.e. few monomers) and the molecular (i.e. entire chain) level. Results are presented as averages quantities over the entire polymer film, as well as, in layers of increasing distance from the graphene surface.

Segmental Dynamics

We start the analysis of the segmental dynamics by monitoring the time evolution of $P_2(t)$ for a vector defined in the monomer level. Here we have used one (backbone) vector for PE and two vectors (one along the backbone and one from the backbone to the side group) for PS and PMMA. All different vectors are shown in Figure 1, drawn on corresponding oligomers of the model systems. A first comparison among the three polymers concerns the backbone 1-3 characteristic vector (v_{1-3}^{BB}), which connects two not consecutive carbon atoms of backbone, separated by one carbon. In Figure 3 the time

autocorrelation functions of $P_2(t)$, of v_{1-3}^{BB} vector, for the three polymer/graphene systems (closed symbols) are depicted, together with the same functions for the corresponding bulk polymer systems (solid lines). These functions describe the average dynamics over the entire film. It is clear that the dynamics of the hybrid polymer/graphene systems is slower than of the corresponding bulk ones; i.e. as expected confinement leads to polymer's retardation. However, this decrease in the mobility of the polymer chains is not the same for all times: In the short time regime $P_2(t)$ curves of hybrid systems are very close to the bulk ones, whereas there is a substantial increase of the difference between these curves at long times, due to a dramatic slowdown of the mobility of the polymer chains of hybrid systems, comparing to the bulk ones. The agreement between the relaxation of the bulk and the hybrid systems at the short time regime is expected, since for these time scales the polymer segments do not feel the interaction with the graphene layers. The differences in the long time regime are due to the much different (qualitatively and quantitatively) relaxation behavior of vectors belonging to adsorbed polymer chains, comparing to vectors which belong to chains in the "bulk" regime of the hybrid system (about the middle of the film), leading to a more complex (average) $P_2(t)$ curve. This phenomenon is certainly more clear for PE, for which simulation time is long enough to capture the full decorrelation of the v_{1-3}^{BB} vector; i.e. $P_2(t)$ reaches the zero value. This aspect will be further discussed below.

Moreover, a considerable quantitative difference in the relaxation time of PE compared to the other two polymers is observed. $P_2(t)$ of v_{1-3}^{BB} characteristic vector is fully decorrelated after just *1ns*, whereas the time autocorrelation functions for the other two polymers have significant values at that time. In addition, $P_2(t)$ for PS decorrelates faster than for PMMA. This is expected since, as mentioned before, the difference between the actual temperature and the bulk polymer glass transition temperature of the PE/graphene systems is larger than that of PS/graphene and PMMA/graphene ones. A further prospective behavior is that the shorter the characteristic vector the longer the relaxation time. This has been justified by calculating the relaxation of v_{1-2}^{BB} (i.e. consecutive carbon atoms of backbone) and of v_{1-4}^{BB} (i.e. not consecutive carbon atoms of

backbone, separated by two carbons) vectors for all polymers studied here (data not shown here). In the rest paper we refer to v_{1-3}^{BB} as the backbone vector.

Furthermore, for PS and PMMA one characteristic vector between the backbone and a side group has been defined in order to study the mobility (relaxation) of the side group (see Figure 1). For PS this vector connects a carbon attached to the backbone and a carbon which belongs to the phenyl group (v^{BPH}) and for PMMA it is defined between the backbone's carbon, connected to the carboxyl side group, and the carboxyl oxygen (v^{BC}). In Figures 4a and 4b a comparison of $P_2(t)$ of the backbone's characteristic vector (v_{1-3}^{BB}) with the characteristic vector of the side group (v^{BPH} or v^{BC}) for PS and PMMA respectively, indicate a slower relaxation of backbone in both cases. This is an expected behavior because the motion of the side group is less constrained than the backbone's motion. Figure 4c presents a comparison of the characteristic vectors of the side groups between PS and PMMA. Data of the corresponding bulk systems are also included and indicate again, that the relaxation of bulk systems is faster than that of the confined systems. Moreover, a faster decorrelation of v^{BPH} compared to v^{BC} is observed, though with smaller difference than the one which stands for the corresponding backbone vectors (this result is also apparent in the second column of Table 2 which is described in the following). The decrease of the difference in the mobility between PS and PMMA side group vectors, compared to the corresponding backbone vectors, can be attributed to the larger flexibility of the v^{BC} vector of PMMA, unlike to v^{BPH} vector of PS, i.e., rotation of v^{BPH} vector is restricted because all atoms of the bulky side group (phenyl ring) have to rotate together. Finally, it is again clear from Figure 4c, the slowdown of the mobility of the v^{BPH} (v^{BC}) vector of PS (PMMA)/graphene systems at long times, similar to the v_{1-3}^{BB} one, shown above in Figure 3. Note that qualitatively similar results for polybutadiene/graphite systems have been recently observed in the literature.[20]

A quantification of the segmental dynamics of the different polymers can be made by defining characteristic relaxation times, based on a fit of the $P_2(t)$ curves with stretch exponential functions (Kohlrausch-Williams-Watts, (KWW))[45] of the form:

$$P_2(t) = A\exp\left[-\left(\frac{t}{\tau_{KWW}}\right)^{\beta}\right],$$

where, A is a pre-exponential factor which takes into account relaxation processes at very short times (i.e., bond vibrations and angle librations), τ_{KWW} is the KWW relaxation time and β the stretch exponent, which takes into account the deviation from the ideal Debye behavior.[46] In all model polymer/graphene systems $P_2(t)$ cannot be fitted well with a single KWW function for all time regimes, due to the complex dynamical behavior at long times, discussed above. This is revealed in the PE curve of Figure 3 and will become more pronounced later, in the analysis of the polymer dynamics as a function of distance from the graphene layer. Therefore, for PE (Figure 3) fitting is restricted to shorter times from *0.5ns* to *20ns*. The shoulder, which is observed in this curve at long times, indicates the existence of more than one relaxation processes in the PE film and can be attributed to the strong attraction of polymer from the graphene layer, at very close distances. Table 2 contains the fitting parameters of all curves for both Figures 3 and 4 which are in agreement with our previous discussion. The comparison of τ_{KWW} for the backbone's characteristic vector among the three polymer/graphene systems makes clear that PE is substantially faster than the other two polymers, while PMMA is about one order of magnitude slower than PS. On the other hand, for side group vectors the difference is decreased i.e., v^{BC} vector of PMMA relaxes about *3* times slower than v^{BPH} vector of PS. Comparisons in relaxation times among bulk systems show a smaller difference between PS and PMMA backbone vector, while the rest vectors' correlations are almost the same with the respective ones of the hybrid systems. Overall, all bulk vectors relax faster than the corresponding polymer/graphene vectors.

The above results refer to averages over the whole polymer film; i.e. they are not a detailed analysis of the non-homogeneous diffusion processes as a function of distance from the graphene layers. However, it is clear that such systems would further expect to exhibit (spatial) dynamic heterogeneity due to the presence of the graphene layers. Therefore, in the following we analyze simulation data as a function of the distance from the graphene layer. The different distances are determined from the density profiles of Figure 2 and adsorption layers are defined. The high peak near the graphene surface

which is followed by one or more, substantially lower peaks, allow us to define adsorption layers as a function of the distance from the surface, while the intermediate (bulk) region is divided into equal spaced layers. A snapshot of PS (with center of mass of each chain in the simulation box), as it is elaborated in the current analysis, is depicted in Figure 5. Different colors correspond to the amount of polymer which lies in each adsorption layer. Note that in order to be consistent in the analysis of the dynamics data, we have calculated $P_2(t)$ for the various characteristic vectors in all adsorption layers, collecting information only from the time periods that the center of mass of the vector is found within the specific adsorption layer. In Figures 6a, 6b and 6c the autocorrelation functions of ν_{1-3}^{BB} for PS, PMMA and PE respectively are presented at the different adsorption layers. Each curve corresponds to an adsorption layer and arrows' direction denotes the increasing distance from graphene. Qualitatively the overall picture exhibits, as expected, some similar characteristics: Polymer segments (vectors) close to graphene relax much slower than segments far away from it, with the differences gradually decaying. The segments far enough from the graphene layer exhibiting a "bulk-like" behavior. However, there are also clear (quantitative and qualitative) differences between the relaxation of the backbone vector for the different polymers. In more detail, for PS the slower dynamics of the segments close to the graphene decays within the first *3-4* adsorption layers gradually approaching the bulk behavior at longer distances, where all curves overlap. For PMMA the relaxation of the backbone vector is gradual only for the first two adsorption layers, while for the rest curves there is an abrupt jump to a faster relaxation rate. Finally, PE chains show a slightly different behavior; the relaxation rate in the first adsorption layer is considerably slower than the rest layers. The well-ordered structure of PE in this layer is responsible for this diversification.

To quantitatively compare the above data, a fit of $P_2(t)$ (of ν_{1-3}^{BB}) curves with KWW stretch exponential functions has been performed for all these curves. Then the segmental relaxation time is calculated as the integral of the KWW curves through the relation: $\tau_{seg} = \frac{\tau_{KWW}}{\beta}\Gamma\left(\frac{1}{\beta}\right)$ where $\Gamma()$ is the gamma function. Note also that for adsorbed PE chains, in order to obtain accurate data, we restrict the fit of the first curve in a small time

window in the range of [*0.01-1*]*ns*. Moreover, in the second adsorption layer, the curve's shape is not the one of a single KWW function. Although the width of this layer is small (*~4nm*) it seems that more than one processes take place in this. Fitting of this curve is also restricted to short times, in this case (up to *0.03ns*). The rest curves are in the bulk region. The side group characteristic vectors of PS and PMMA (data not shown here) present a diversification similar to the one of the corresponding backbone vectors. Data for τ_{seg} and β for the three systems are presented in Figures 7a and 7b, as a function of distance from the graphene layer for v_{1-3}^{BB} characteristic vector. A rough estimation of the error bars are ±[*0.05-0.1*] for β and of the order of [*20%-30%*] of the actual value for τ_{seg}. These errors are in general smaller in the bulk region and become larger close to the surface. Note here that τ_{KWW} (and consequently τ_{seg}) values are very high for both PMMA and PS in the first adsorption layer and their error bars are also very large. These times are larger than the time window of the simulation and cannot be accurately predicted by the current simulations. Therefore, we use these values more as a rough estimation of the slowdown of the chain dynamics close to the graphene layers and not as accurate absolute numbers. For this reason we use a different (open) symbol in the corresponding graphs for all these values.

Figure 7a confirms the above discussion for the relaxation rates of the different polymers. Relaxation times attain the lowest values for PE and the highest ones for PMMA, while PS is an intermediate case for all adsorption layers. For all polymers the segmental relaxation time decreases with the distance from the surface reaching to a constant value, very close to the one of the corresponding bulk system (horizontal dashed lines). Moreover, Figure 7a provides a quantification of the time differences among the three polymers which, in the bulk region, is $\sim 3x10^3$ for PS/PE and *~10* for PMMA/PS. It is interesting to observe that for PE there is a large jump in the segmental relaxation time between the first adsorption layer and the rest film. Very close to graphene, up to *0.6nm*, PE has substantially slower dynamics, with τ_{seg} *~10ns*, due to the well-ordered layered structure which is formed at these distances, whereas at longer distances τ_{seg} is in the range of [$2x10^{-2}$-$5x10^{-3}$]*ns*. Note that the segmental dynamics of PE reaches its actual bulk value at distances ~ *2nm*, whereas PMMA and PS at about ~ *3nm*. A possible

reason for the difference in the width of the polymer/graphene interface, defined through the segmental dynamics, might be the existence of side groups in PS and PMMA whose extent is of the order of *~0.5nm*. A further investigation of this issue will be the subject of a future work.

The values of β exponents are depicted in Figure 7b. For all systems β values increase with the distance from the surface. This observation indicates that the existence of the graphene layer leads systems to larger deviations from the ideal Debye behavior (i.e., wider distribution of relaxation times). Furthermore, β exponents for all three polymers, reach their distance-independent "bulk-like" values, beyond the same range of distances about *~2-4nm*, given the statistical uncertainty, similar to the distance shown for the τ_{seg} values presented above. We should also state here the complex character of the chain dynamics close to the solid (graphene) layers; i.e. not only the average relaxation times, but also their distributions, are different. A more detailed investigation of the full distribution of relaxation times as a function of distance from the graphene layers is under investigation.

A comparison of the segmental relaxation times between the side groups of PS and PMMA is depicted in Figure 8a for v^{BPH} and v^{BC} vectors respectively. A behavior similar to the one of the backbone vectors for the two polymers is observed (i.e, PS relaxes faster than PMMA). However, there is a decrease in the difference of the segmental relaxation times of the side group vectors, between the two polymers, compared to the corresponding difference of the backbone vectors, which has been mentioned previously as well. The analysis in layers of increasing distance from graphene makes clear that in the second adsorption layer $\tau_{segm.}$ attains almost the same values for the two polymers, whereas in the bulk region there is a small and almost constant difference, which renders v^{BPH} faster than v^{BC}. The reason for this decrease is the fact that the relaxation of side groups is determined by two competing factors; the one is the faster total dynamics of PS compared to PMMA, while the other is the more restricted motion of the phenyl ring of PS, in order to retain its shape, compared to the carboxyl side group of PMMA. Therefore, this competition diminishes the difference in τ_{seg} values, though the first is the predominant factor. On top of that, the effect of the

graphene layer plays a crucial role on this competition. The corresponding β values, which are depicted in Figure 8b, are almost equal at any distance from graphene, except from the first adsorption layer, where we have values of high uncertainty. In the bulk region β values are close to *0.5* for both vectors just as the corresponding values for the bulk systems, within the error bars. In addition, the segmental relaxation times, defined through the v^{BPH} and v^{BC} vectors for PS and PMMA respectively also reach their actual bulk values at distances of about ~ *3-4nm* from the graphene layers in agreement with the relaxation behavior of the v_{1-3}^{BB} vector.

Finally, a comparison of the relaxation times between the backbone and the corresponding side group has been made for PS and PMMA polymers. The ratios of the segmental relaxation times $\tau_{seg}^{v^{BPH}} / \tau_{seg}^{v_{1-3}^{BB}}$ and $\tau_{seg}^{v^{BC}} / \tau_{seg}^{v_{1-3}^{BB}}$ for PS and PMMA respectively have been calculated, at all adsorption layers (data not shown here). In both cases the side group relaxes faster than the backbone's vector however, the difference is greater in PMMA. Beyond the first adsorption layer, for which the statistics is not accurate enough, this ratio attains an almost constant value for each polymer; $\frac{\tau_{seg}^{v^{BPH}}}{\tau_{seg}^{v_{1-3}^{BB}}} \approx 0.7$ for PS, whereas $\frac{\tau_{seg}^{v^{BC}}}{\tau_{seg}^{v_{1-3}^{BB}}} \approx 0.2$ for PMMA. The smaller value for PMMA is to be expected since, as mentioned above, the side group of it is much more flexible than the one of PS.

Having explored the mobility of polymer chains in the segmental level, we'll continue our calculations at a longer length scale (i.e. the molecular level).

Chain Dynamics

Orientational Dynamics. In the following results relating to terminal-chain dynamics are presented. A characteristic quantity of molecular level is the end – to – end distance, $\mathbf{R_{ee}}(t)$. The calculation of the end-to-end vector autocorrelation function, defined as: $u(t) = \frac{\langle \mathbf{R}_{ee}(t) \bullet \mathbf{R}_{ee}(0) \rangle}{\langle R_{ee}^2 \rangle_0}$, provides information for the orientational dynamics in the entire chain level. $R_{ee}(t)$ and $R_{ee}(0)$ are the end-to-end distances at time *t* and *0*

respectively, and $\left\langle R_{ee}^2 \right\rangle_0$ is the mean squared value of the equilibrium (unperturbed) end-to-end distance. Figure 9 contains the average time autocorrelation function ($u(t)$), over the entire polymer film, for the three systems. Data for the corresponding bulk systems (solid lines) are also included. Qualitatively the picture is similar to the one observed before for the segmental dynamics: The relaxation of the end-to-end vector of the hybrid interfacial systems is slower than that of the corresponding bulk ones, whereas PMMA has the slowest terminal dynamics while PE has the fastest one, in agreement with our observations in the segmental level. It is further interesting to observe a small shoulder in the PE curve of Figure 9, similar to that of Figure 3, which is a result of the strong attraction of polymer from the graphene layer, at very close distances (i.e., first adsorption layer). The parameters of the fit of $u(t)$ curves with KWW functions are contained in Table 2. For the PE curve fit is restricted to shorter times, up to *~0.1ns*.

We continue with an analysis of $u(t)$ at different adsorption layers. Note here that for all calculations in the molecular level we have defined wider adsorption layers with respect to graphene compared to the previous analysis of the segmental dynamics. This makes sense if we consider that the dynamics of the polymer chain is affected by segments along the whole chain which might belong to different layers. Therefore, and in order to also improve statistics, we analyze polymer chain data every *10Å* for the first and the second layers, while the rest of them correspond to *20Å*. Moreover, their width is the same for the three polymers. At the entire chain level, the integral of the KWW curves defines the molecular chain end-to-end vector relaxation time ($\tau_{mol}^{R_{ee}}$). The molecular relaxation time together with the stretching exponent β, are depicted in Figure 10a and 10b as a function of the distance from the surface. Data in Figure 10a has shown the dramatic increase of $\tau_{mol}^{R_{ee}}$ close to the graphene layer, compared to corresponding bulk values, shown with dashed lines. Furthermore, a slight difference in the distance at which the $\tau_{mol}^{R_{ee}}$ reaches the plateau distance-independent bulk value is observed: for PE is about ~ *2nm*, whereas for PMMA and PS is about *3-4nm*, in agreement to the data found from the orientational segmental relaxation time. The very large difference in relaxation times between PE and the other two polymers is again obvious. The β exponent for PE and PS

reaches to a constant value at the bulk region, which is almost equal to *0.95* for PE and *0.84* for PS (i.e., equal to the values of the corresponding bulk systems in the range of the statistical uncertainty). However, in PMMA β is an increasing function of the distance from graphene, which gradually tends to a plateau value of almost *0.77* (i.e., very close to the one which stands for the corresponding bulk system). These values show that in the bulk region PMMA has the wider distribution of relaxation times, PS follows and PE has the narrower one. Note that according to the Rouse model the relaxation of the end-to-end vector should be described through a sum of exponentials. Deviations from this behavior observed here are to be expected, since the molecular lengths studied here are much smaller than those for which the Rouse model would expect to be valid; i.e. the statistics Gaussian and the monomeric friction coefficient constant.[47]

Translational Dynamics. The translational dynamics of polymers, in the entire chain level, can be studied through the mean squared displacement, for the chain-center-of mass, given through: $\Delta R^2_{CM} = \left\langle \left(R_{CM}(t) - R_{CM}(0) \right)^2 \right\rangle$, where R_{CM} is the position of the chain's center of mass. In what follows we have calculated mean squared displacements both for in plane motion (i.e., *xy*-component) and normal to the surface (i.e., *z*-component), as a function of the distance from graphene. First the parallel to the graphene layer dynamics (ΔR^2_{xy}) is presented in Figure 11 for PE chains of the PE/graphene system in the different layers. The corresponding data of bulk PE are presented with dashed lines. For the very short times the dynamics for all segments is as expected similar (ballistic motion). Then the chain dynamics at longer times follows closely the dynamics of the bulk unconstrained system. Only for the chains belonging in the first layer there is a small decrease in the mobility for times from $10^{-3}ns$ to $10^{-1}ns$. Overall the chain center-of-mass xy-dynamics is almost homogeneous at any distance, identical to the diffusion (*xy*-component) of the corresponding bulk system, for all but the first adsorption layer. The behavior is qualitatively similar for the other two polymers (data not shown here).

Second, in Figure 12 the *z*-component of the mean squared displacement (ΔR^2_z) is depicted for all three polymers. The arrow's direction indicates the increasing distance from graphene. Again, for short distances all curves are as expected on top of each other, since they do not "feel" the effect of the graphene layers. But, on top of that, Figure 12

reveals the range of the effect of graphene on the mobility of the whole polymer chain. Within the first *10Å* the attraction from graphene hinders mobility and for none of the three polymers $\langle \Delta R_z^2 \rangle$ exceeds $1Å^2$. For the next *10Å*, and as the attraction is reduced, the differences among the polymers are enhanced. Beyond *20Å* dynamics is identical for the rest of the film, though different among the polymers. It is interesting to observe that only for PE $\langle \Delta R_z^2 \rangle$ attains a plateau value in the bulk regime (i.e., beyond *20Å*) and this happens after just *1ns*. The other two polymers have not reached to a plateau value during their simulation times (i.e. ~ *0.5μs*). The plateau is induced from the restriction of analysis in layers of specific width and only PE, which is considerably faster than the other two polymers, has enough time to obtain constant motion within the layer. The corresponding bulk curves (dashed lines) are also included in Figure 12 and coincide with the curves of the last three adsorption layers, which lie in the bulk region, though for PE there is a deviation beyond *0.1ns*, due to the plateau region. The quantitative differences in the mean squared displacements among the three polymers are expected in agreement with our previous analysis. A plateau like regime is observed for PS, but more pronounced for PMMA, from time 10^{-2} to *10 ns*, which indicates a glassy like behavior in the first two adsorption layers (i.e., up to *2nm*) for the specific time period.

In order to further quantify the effect of graphene on the mobility of the polymer chains, as a function of the distance from the graphene layers, we define an effective time dependent self-diffusion coefficient along the confinement (z) dimension, $D_z(t)$ through:

$$D_z(t) = \frac{\left\langle \left(R_z(t) - R_z(0) \right)^2 \right\rangle}{6t}$$

Note that for a homogeneous molecular system, exhibiting linear (Fickian) diffusion, $D_z(t)$ reaches a constant time independent value (self-diffusion coefficient), for times longer than about the maximum relaxation time of the molecule (polymer chain). Here since the diffusion along the confinement (z-dimension) is not linear we define an apparent diffusion coefficient, $D_z(\tau_c)$ through a characteristic "observation" time scale, τ_c.[13] Values of τ_c were chosen in order to represent the relaxation time of ν_{1-3}^{BB} vector for each polymer respectively. The insets of Figure 12 present the ratio of $D_z(\tau_c)$ over the corresponding bulk diffusion coefficient for each polymer, at the specific time τ_c, as a

function of the distance from the graphene layer. A comparison among the insets makes clear the different way that graphene affects polymers dynamics at different distances from it. There is an obvious diversification of PE, compared to the other two polymers, where the effect of the graphene layer attenuates abruptly beyond *10Å*, while it is still strong up to *20Å* for PS and PMMA. Then $D_z(\tau_c)$ approximates gradually D_{zBULK} for all three systems, though in a different rate. Diffusion in the chain center-of-mass level reaches its bulk value at distances of about *~4nm* for PE and *6-8nm* for PS and PMMA.

4 Conclusions

In the present work we have explored the effect of graphene on the mobility of polymers, by studying three well known and widely used polymers, polyethylene (PE), polystyrene (PS) and poly(methyl-methacrylate) (PMMA). In more detail, three hybrid polymer/graphene interfacial systems of similar molecular chain size, $<R_g>$, were studied through atomistic MD simulations. The film thickness for all systems was in the range of [*19-23*]$<R_g>$. The corresponding bulk systems were simulated as well. We explored the dynamics of polymer chains both in the segmental and the molecular level and we quantified the differences in relaxation times among the polymers. In addition to the study of the average dynamics over the entire polymer film, a detailed analysis of the dynamics as a function of the distance from the surface has been performed. Comparisons were made both among the three polymer/graphene systems and between the hybrid and the corresponding bulk system.

Segmental analysis was based on the time autocorrelation functions $P_2(t)$ (i.e., the second Legendre polynomials) for two types of vectors, one along the backbone of the polymer chain and another from the backbone to a side group, for PS and PMMA only. v_{1-3}^{BB} is a common vector for the three polymers, which connects two non-consecutive carbon atoms of the backbone, separated by one carbon. Fitting of the above functions with KWW functions provide information for both segmental relaxation times, τ_{seg} and stretch exponents, β. In all cases bulk systems are faster. This observation renders the existence of the graphene layer a reason for the reduction in polymer mobility. An interesting issue is the extent of this effect and the way that it diversifies among the three

polymers. A comparison of the segmental relaxation times among the three polymers revealed that PE is much faster than the other two polymers. The difference of the actual temperature from the glass transition temperature, T_g, of each system, corroborates this behavior. As a function of the distance from the graphene layer τ_{seg} attains large values close to the surface, which decrease as the distance increases, reaching to a plateau value in the bulk region, identical to the value which stands for the corresponding bulk systems. A remarkable observation here is the abrupt jump in τ_{seg} values of PE between the first and the rest adsorption layer, which covers almost two orders of magnitude in *ns*. This is due to the well-ordered layered structure that PE forms very close to the graphene layer, which causes a substantial retardation in its dynamics. For the two other polymers there is a gradual decrease with the distance, though the values for the first adsorption layer are of high uncertainty. β-values indicate a wider distribution of polymer segmental relaxation times close to graphene layers, whereas in the bulk region all three systems attain almost the same values, in the range of the statistical uncertainty. The relaxation of the side group vectors is faster than the corresponding backbone vectors for PS and PMMA, due to the fact that their motion is less restricted compared to a backbone vector. Moreover, v^{BPH} and v^{BC} have almost the same segmental relaxation times up *~3nm* from the graphene, while at longer distances PS is faster than PMMA though with a smaller difference than the corresponding bulk vectors. This is a combined result of the faster dynamics of PS, but at the same time of the more restricted motion of v^{BPH} compared to v^{BC}, due to the phenyl ring and of the effect of the graphene layer.

Concerning to longer length scales we explore chain dynamics through the calculation of the end-to-end autocorrelation function, $u(t)$. The correlations in molecular relaxation times, $\tau_{mol}^{R_{ee}}$, among the three polymers, are qualitatively the same with the segmental relaxation times for v_{1-3}^{BB}. However, there is a considerable quantitative difference between them, which renders $\tau_{mol}^{R_{ee}}$ longer than τ_{seg}, as expected. This difference is bigger close to the graphene layer and it is more pronounced for PMMA.

Finally, the in-plane motion (*xy*) and normal to the plane motion (*z*), of the center of mass of the polymer chain has been studied through the calculation of the mean squared displacement. In plane motion, found to be unaffected by the existence of the graphene layer, for all three polymers, except for a small retardation, which is observed in the first adsorption layer. The effect of the graphene layer is extended up to *2nm* on the *z*-component of the mean squared displacement, while beyond this, diffusion is identical to that of the corresponding bulk system. The large gap in $\langle \Delta R_z^2 \rangle$ between the first and the second adsorption layer of PE is a result of its well-ordered layered structure close to graphene. Moreover, the considerably higher mobility of PE compared to PS and PMMA is the reason for the plateau, which is formed in $\langle \Delta R_z^2 \rangle$ curves as a result of our analysis in adsorption layers.

Overall, despite the similarities of the different polymers studied here and the fact that for all of them the polymer/graphene interaction is dominated by dispersion van der Waals forces there are clear (qualitative and quantitative) differences in the dynamic properties of the polymer chains in particular at the polymer/graphene interface. Furthermore, the width of the polymer/graphene interface depends, as expected, on the actual property in which it is defined. Note that simulation data shown here represent a rather ideal system, in which single graphene layers are ideally dispersed in the polymer matrix. In more realistic systems the graphene phase corresponds to graphene layers dispersed in the polymer matrix, in which quite often there are multiple graphene layers stacked together. The dependence of the polymer properties as a function of the number of graphene layers is under investigation.

Current work is related to the study of the effect of the polymer matrix on the properties of the graphene layers. For this work a model with full energetic interactions among the carbon atoms of graphene is required. Preliminary results for the polymer chains are very similar to the data presented here. Furthermore, the study of longer polymer chains is under investigation through a rigorous hierarchical multi-scale methodology similar to the one followed recently for polymer/metal systems.[30,48]

Aknowledgments

We would like to thank Manolis Doxastakis for valuable discussions. A.R. acknowledges partially support by the European Union's Seventh Framework Programme (FP7-REGPOT-2009-1) project Archimedes Center for Modeling, Analysis and Computation under Grant No. 245749 as well as "FORTH Graphene Centre". This research has been co-financed by the European Union (European Social Fund - ESF) and Greek national funds through the Operational Program "Education and Lifelong Learning" of the National Strategic Reference Framework (NSRF) - Research Funding Program: THALES.

Table 1

Number of Polymer Chains and Film Thickness for the PS the PMMA and the PE systems.

System	*N*	*d(nm)*
PMMA	135	13.35
Bulk PMMA	54	-
PS	120	13.67
Bulk PS	56	-
PE	420	13.91
Bulk PE	420	-

Table 2

Relaxation times τ_{KWW}, stretch exponents β, and pre-exponential factors A, for the hybrid polymer (PS, PMMA, PE)/graphene systems and the corresponding bulk polymers.

System/vector	τ_{KWW}*(ns)*	$\tau_{KWW}(ns)_{BUKL}$	β	β_{BUKL}	A	A_{BULK}
PMMA/ v^{BB}1-3	112.04	41.12	0.46	0.56	0.97	0.95
PS /v^{BB}1-3	14.36	8.12	0.50	0.66	0.94	0.92
PE/v^{BB}1-3	0.004	0.003	0.56	0.53	1	1
PMMA/ v^{BC}	21.83	9.40	0.38	0.50	0.92	0.88
PS/v^{BPH}	6.51	3.99	0.35	0.59	0.9	0.81
PMMA/ *u(t)*	1848.79	604.07	0.67	0.72	0.99	0.98
PS/ *u(t)*	91.55	57.95	0.74	0.87	0.97	0.96
PE/ *u(t)*	0.085	0.065	0.84	0.93	0.999	0.98

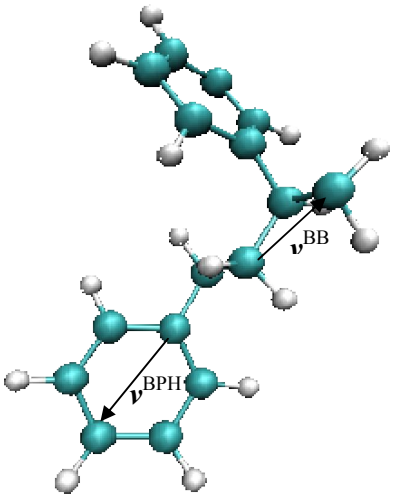

(a) PS

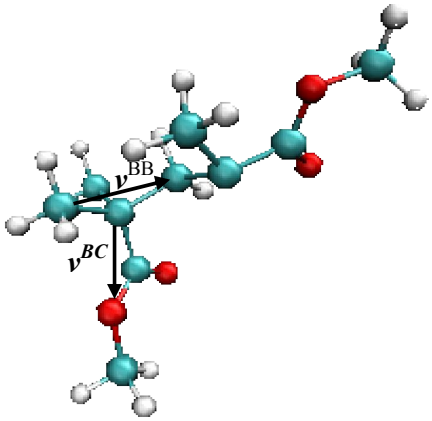

(b) PMMA

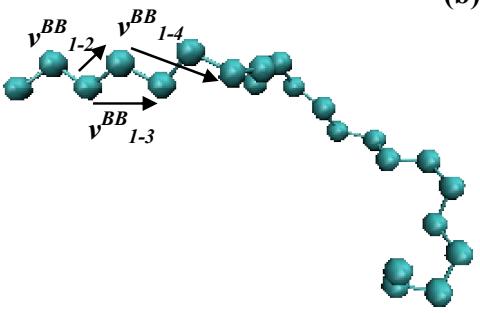

(c) PE

Figure 1

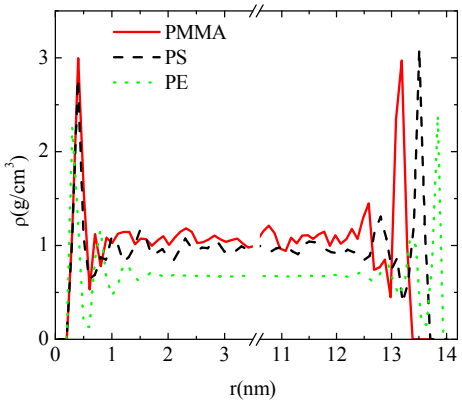

Figure 2

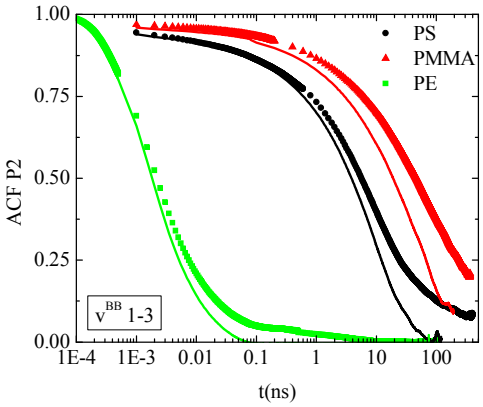
1.00
0.75
0.50
0.25
0.00
ACF P2
1E-4
1E-3
0.01
0.1
1
10
100
t(ns)
PS
PMMA
PE
v^BB 1-3

Figure 3

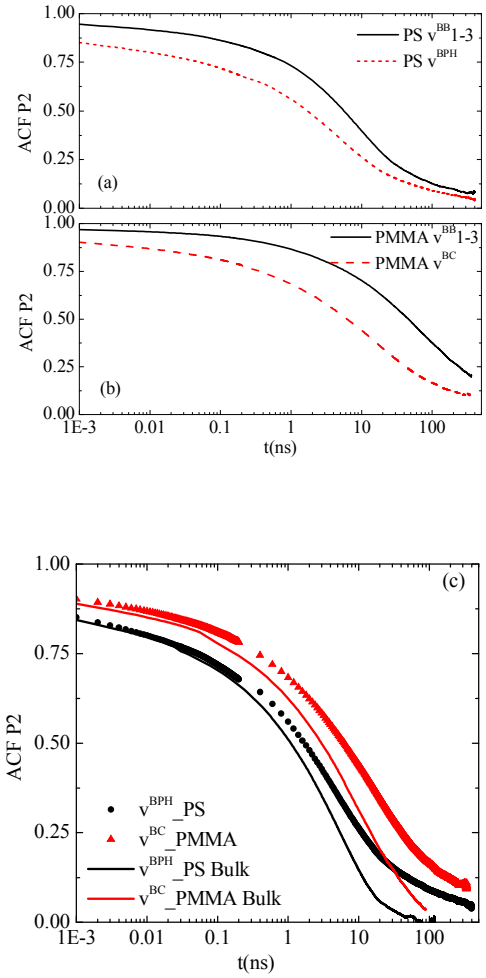
1.00
0.75
0.50
0.25
0.00
ACF P2
PS v^BB1-3
PS v^BPH
(a)
PMMA v^BB1-3
PMMA v^BC
(b)
1E-3
0.01
0.1
1
10
100
t(ns)
(c)
v^BPH_PS
v^BC_PMMA
v^BPH_PS Bulk
v^BC_PMMA Bulk

Figure 4

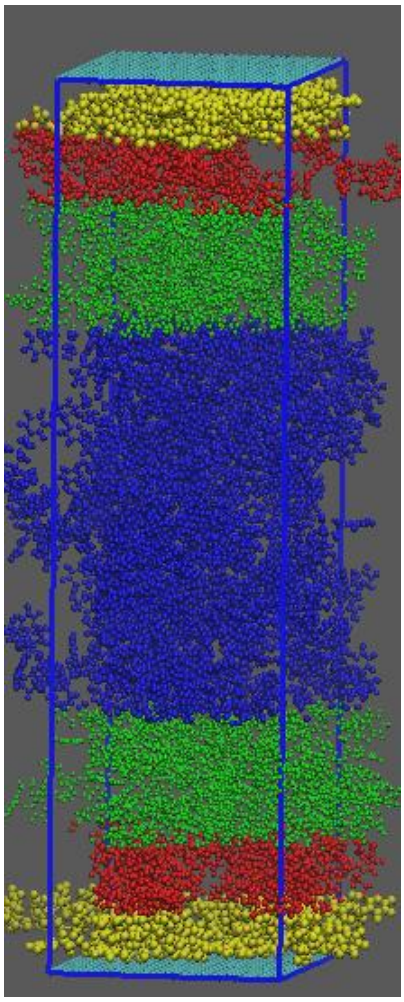

Figure 5

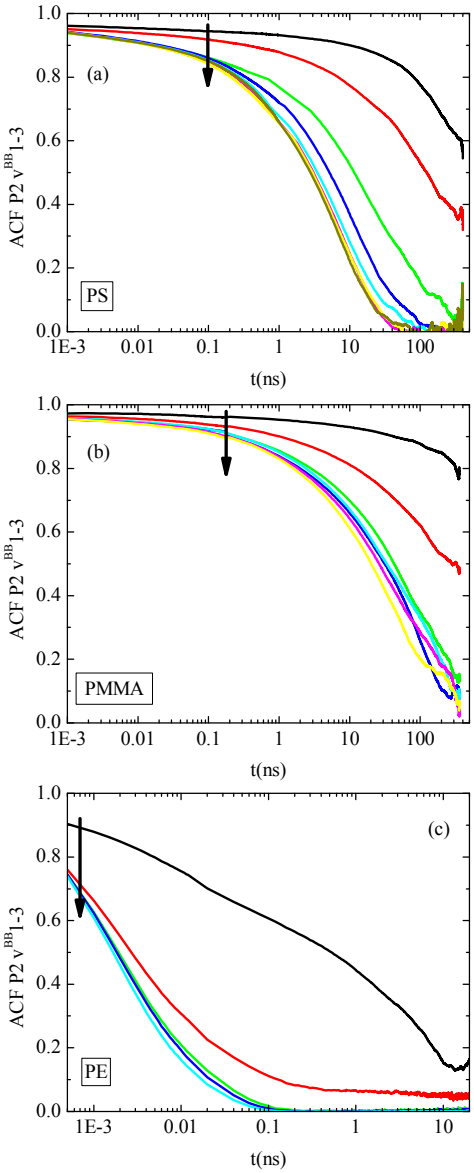
(a)
PS
(b)
PMMA
(c)
PE
ACF P2 v^BB 1-3
t(ns)
1.0
0.8
0.6
0.4
0.2
0.0
1E-3
0.01
0.1
1
10
100

Figure 6

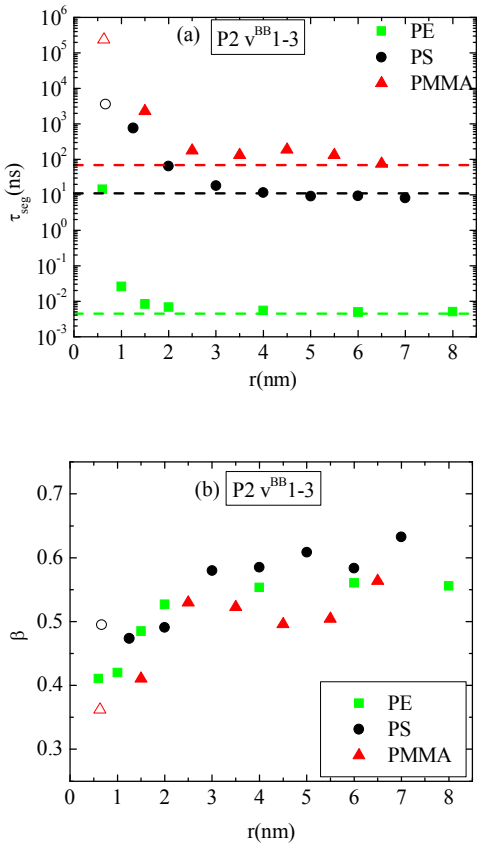

Figure 7

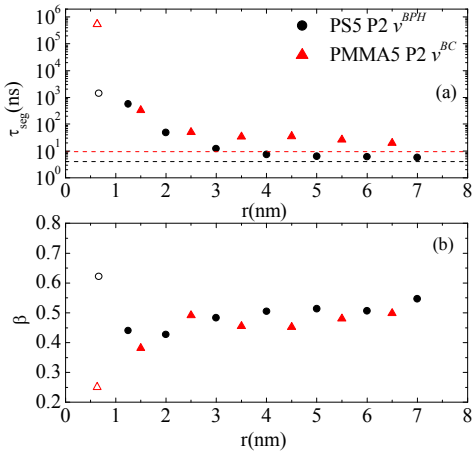

Figure 8

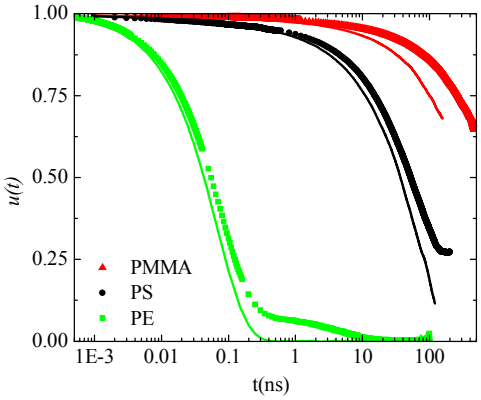

Figure 9

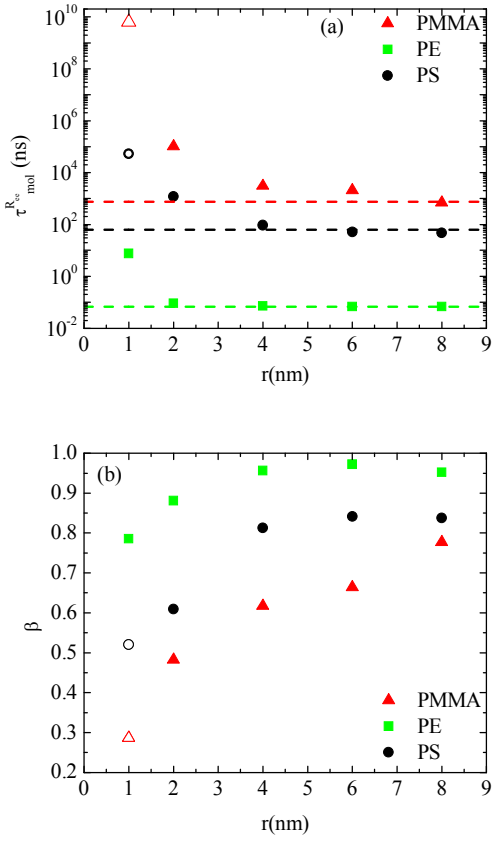

Figure 10

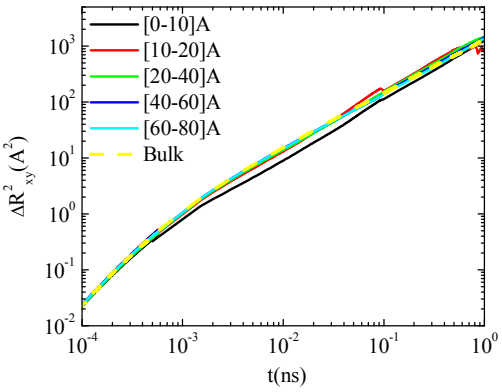

Figure 11

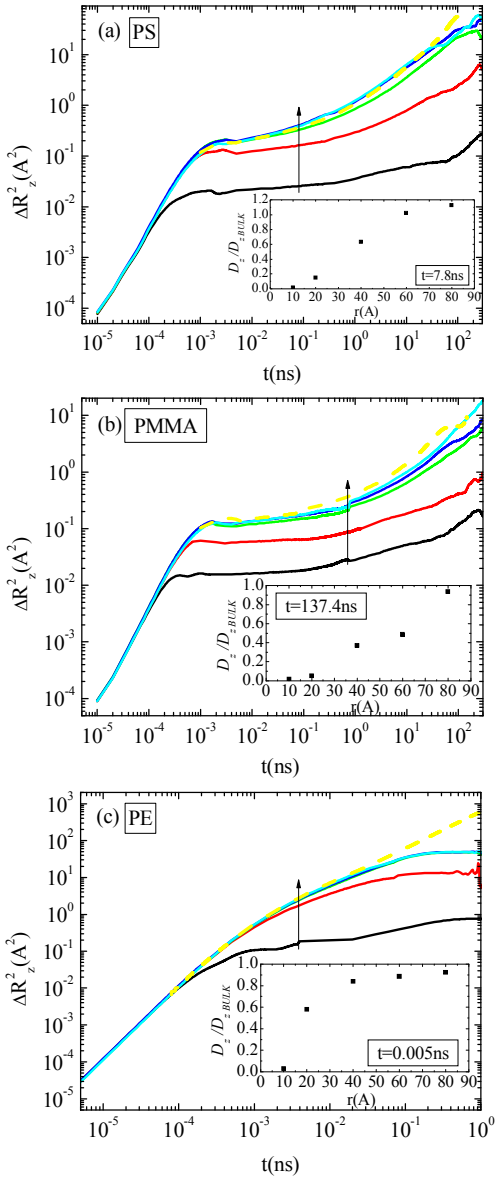
(a) PS
$\Delta R_z^2 (A^2)$
t(ns)
$D_z/D_{z\,BULK}$
r(A)
t=7.8ns
(b) PMMA
$\Delta R_z^2 (A^2)$
t(ns)
$D_z/D_{z\,BULK}$
r(A)
t=137.4ns
(c) PE
$\Delta R_z^2 (A^2)$
t(ns)
$D_z/D_{z\,BULK}$
r(A)
t=0.005ns

Figure 12

Figure Captions

Fig. 1: Snapshots of oligomers of (a) PS, (b) PMMA and (c) PE chains. Characteristic vectors along the backbone and from the backbone to the side groups are drawn.

Fig. 2: Monomer density profiles as a function of distance from graphene layers for PS, PMMA and PE hybrid polymer/graphene systems.

Fig. 3: Time autocorrelation function of bond order parameter $P_2(t)$ for the backbone characteristic vector v_{1-3}^{BB} of PS, PMMA and PE polymer/graphene systems (closed symbols) and of the corresponding bulk systems (solid lines). Values are averages over the entire polymer film.

Fig. 4: Comparison of time autocorrelation functions of bond order parameter $P_2(t)$ (a) between the backbone characteristic vector v_{1-3}^{BB} and the side group characteristic vector v^{BPH} of PS, (b) between the backbone characteristic vector v_{1-3}^{BB} and the side group characteristic vector v^{BC} of PMMA and (c) between the side group characteristic vectors of PS and PMMA of the confided (closed symbols) and corresponding bulk systems (solid lines). Values are averages over the entire polymer film.

Fig. 5: A snapshot of PS/graphene model system. Different colors correspond to different adsorption layers with respect to the surface.

Fig. 6: Time autocorrelation function of bond order parameter $P_2(t)$ for the backbone characteristic vector v_{1-3}^{BB} at different distances (adsorption layers) from graphene (a) PS, (b) PMMA and (c) PE.

Fig. 7: (a) Segmental relaxation time of the backbone characteristic vector v_{1-3}^{BB}, based on $P_2(t)$ time autocorrelation function, for PS, PMMA and PE hybrid polymer/graphene systems as a function of the distance from graphene. Dashed lines represent the values for

the segmental relaxation times of the corresponding bulk systems. (b) The stretch exponent β, as extracted from the fit with KWW functions for the three systems.

Fig. 8: (a) Segmental relaxation time of the side group characteristic vectors, v^{BPH} for PS and v^{BC} for PMMA, based on $P_2(t)$ time autocorrelation function as a function of the distance from graphene. Dashed lines represent the values for the segmental relaxation times of the corresponding bulk systems. (b) The corresponding stretch exponents β, as extracted from the fit with KWW functions.

Fig. 9: Time autocorrelation function $u(t)$ of the end-to-end characteristic vector $R_{ee}(t)$ of PS, PMMA and PE polymer/graphene systems (closed symbols) and of the corresponding bulk systems (solid lines). Values are averages over the entire polymer film.

Fig. 10: (a) Molecular relaxation time of the end-to-end characteristic vector $R_{ee}(t)$, based on $P_1(t)$ time autocorrelation function, for PS, PMMA and PE hybrid polymer/graphene systems as a function of the distance from graphene. Dashed lines represent the values for the molecular relaxation times of the corresponding bulk systems. (b) The stretch exponent β, as extracted from the fit with KWW functions for the three systems.

Fig. 11: The *xy*-component of the mean squared displacement as a function of time, at different distances from graphene for the PE/graphene system (in plane motion).

Fig. 12: The *z*-component of the mean squared displacement as a function of time, at different distances from graphene for (a) PS/graphene, (b) PMMA/graphene and (c) PE/graphene systems. The direction of the arrow indicates the increasing distance from the surface. The insets present the ratio of the time dependent self-diffusion coefficient along *z*, $D_z(\tau_c)$, at a specific time τ_c, over the corresponding bulk diffusion coefficient for each polymer, as a function of the distance from the graphene layer.

[1] K. S. Novoselov, A. K. Geim, S. V. Morozov, D. Jing, Y. Zhang, S. V. Dubonos, I. V. Grigorieva and A. A. Firsov, *Science*, 2004, **306** (5696), 666.
[2] H. Kim, A. A. Abdala and C. W. Macosko, *Macromolecules*, 2010, **43**, 6515.
[3] C. N. R. Rao, A. K. Sood, K. S. Subrahmanyam and A. Govindaraj, *J Mater Chem*., 2009, **19**(17): 2457.
[4] C. Lv, Q. Xue, D. Xia, M. Ma, J. Xie and H. Chen, *J. Phys. Chem*., 2010, **114**, 6588.
[5] J. R. Potts, D. R. Dreyer, C. W. Bielawski, R. S. Ruoff, *Polymer*, 2011, **52**, 5.
[6] P. M. Ajayan, L.S. Schadler, C. Giannaris, A. Rubio, *Adv. Mater*., 2000, **12**, 750.
[7] N. A. Kotov, *Nature*, 2006, **442**, 254.
[8] A. K. Geim and K. S. Novoselov, *Nature Mater.*, 2007, **6**, 183.
[9] C. Lee, X. Wei, J. W. Kysar, J. Hone, *Science*, 2008, **321**, 385.
[10] H. Kim, C. W. Macosko, *Macromolecules*, 2008, **41**, 3317.
[11] T. Ramanathan, A. A. Abdala, S. Stankovich, D. A. Dikin, M. Herrera-Alonso, R. D. Piner, D. H. Adamson, H. C. Schniepp, X. Chen, R. S. Ruoff, S. T. Nguyen, I. A. Aksay, R. K. Prud'Homme, L. C. Brinson, *Nature Nanotechnol.*, 2008, **3**, 327.
[12] K. F. Mansfield and D. N. Theodorou, *Macromolecules*, 1991, **24**, 4295.
[13] V. A. Harmandaris, K. C. Daoulas and V. G. Mavrantzas, *Macromolecules*, 2005, **38**, 5780; *Macromolecules*, 2005, **38**, 5796.
[14] A. P. Awasthi, D. C. Lagoudas and D. C. Hammerand, *Model Simul Mater Sci Eng*, 2009, **17**, 015002.
[15] L. Yelash, P. Virnau , K. Binder and W. Paul, *Phys. Rev. E*, 2010, **82**, 050801.
[16] Y. B. Tatek and M. Tsige, *J. Chem. Phys*., 2011, **135**, 174708.
[17] J.-S. Yang, C.-L. Yang, M.-S. Wang, B.-D. Chen and X.-G. Ma, *Phys. Chem. Chem. Phys*., 2011, **13**, 15476.
[18] A. N. Rissanou and V. A. Harmandaris, *J. Nanopart. Res.*, 2013, **15**, 1589.
[19] A. N. Rissanou and V. A. Harmandaris, *Macromolecural Symposia*, 2013 (in press).
[20] L. Yelash, P. Virnau , K. Binder, W. Paul, *Europhys. Lett*., 2012, **98**, 28006.
[21] Y. N. Pandey, M. Doxastakis, *J. Chem. Phys.*, 2012, **136**, 094901.
[22] D. Konatham, K. N. D. Bui, D. V. Papavassiliou, A. Striolo, *Molecular Physics*, 2011, **109**, 97.
[23] S. Shenogin, L. Xue, R. Ozisik, P. Keblinski, D. G. Cahill, *J. Appl. Phys*., 2004, **95**, 8136.
[24] H. Yang, Z. Y. Lu, Z. S. Li, C. C. Sun, *J. Mol. Modeling*, 2006, **12,** 432.
[25] H. X. Guo, X. Z. Yang, T. Li, *Phys. Rev. E*, 2000, **61**, 4185.
[26] Zhonghua Ni, Hao Bu, Min Zou, Hong Yi, Kedong Bi, Yunfei Chen, *Physica B*, 2010, **405**, 1301.
[27] R. Rahman, *Journal of Applied Physics*, 2013, **113**, 243503.
[28] T. Matsuda, G. D. Smith, R. G. Winkler and D. Y. Yoon, *Macromolecules*, 1995, **28**, 165.
[29] K. Johnston and V.A. Harmandaris, *Macromolecules*, 2013, **46**, 5741.
[30] K. Johnston, V. Harmandaris, *Soft Matter*, 2013, **9**, 6696.
[31] A. M. Skvortsov, F. A. M. Leermakers, G. J. Fleer, *J. Chem. Phys*., 2013, **139**, 054907.
[32] M. Muller, B. Steinmuller, K. Ch. Daoulas, A. Ramirez-Hernandez, J. J. de Pablo, *Phys. Chem. Chem. Phys*., 2011, **13**, 10491.

[33] G. Bussi, D. Donadio, M. Parinello, *J. Chem. Phys*., 2007, **126**, 014101.
[34] B. Hess, C. Kutzner, D. van der Spoel, E. Lindahl,, *Journal of Chemical Theory and Computation*, 2008, ***4***, 435.
[35] W. L. Jorgensen, D. S. Maxwell, J. Tirado-Rives, *J. Am. Chem. Soc.* 1996, **118**, 11225.
[36] F. Müller-Plathe, *Macromolecules* 1996, ***29***, 4782.
[37] W. A. Steele, *Surf. Sci.* 1973, **36**, 317.
[38] J. Koo, *Polymer Nanocomposites Processing, Characterization, And Applications* **2006**, McGraw-Hill.
[39] W. Wunderlich, In Polymer Handbook, 3rd ed.; Brandrup, J., Immergut, E. H., Eds., John Wiley & Sons: New York, 1989; Sec. 5, p 77.
[40] P. Zoller and D. J. Walsh, Standard Pressure-Volume-Temperature Data for Polymers, Technomic, Lancaster, 1995.
[41] A. N. Rissanou, S. H. Anastasiadis, I. A. Bitsanis, *J. Pol. Sci. B*, 2009, **47**, 2462.
[42] I. A. Bitsanis, G. Hatziioannou, *J. Chem. Phys*., 1990 **92**, 3827.
[43] I. A. Bitsanis, G. ten Brinke, *J. Chem*. *Phys.*, 1993, **99**, 3100.
[44] M. Doxastakis, Y-L. Chen, O. Guzmán, J. J. de Pablo, 2004, *J. Chem. Phys*. **120**, 9335.
[45] G, Williams , D. C. Watts, *Transactions from the Faraday Society*, 1970, **66**, 80.
[46] B. Berne, R. Pekora, Dynamic Light Scattering, John Wiley and Sons, Dover 2000.
[47] V. A. Harmandaris, V. G. Mavrantzas, D. N. Theodorou, *Macromolecules*, 1998, **31**, 7934.
[48] K. Johnston, V. Harmandaris, *Soft Matter*, 2012, **8**, 6320-6332; *J. Phys. Chem. C*, 2011, **115**, 14707.